Journal of Biomedical Optics

SPIEDigitalLibrary.org/jbo

Noncontact diffuse correlation spectroscopy for noninvasive deep tissue blood flow measurement

Yu Lin
Lian He
Yu Shang
Guoqiang Yu

SPIE

Noncontact diffuse correlation spectroscopy for noninvasive deep tissue blood flow measurement

Yu Lin, Lian He, Yu Shang, and Guoqiang Yu
University of Kentucky, Center for Biomedical Engineering, Lexington, Kentucky 40506

Abstract. A noncontact diffuse correlation spectroscopy (DCS) probe has been developed using two separated optical paths for the source and detector. This unique design avoids the interference between the source and detector and allows large source-detector separations for deep tissue blood flow measurements. The noncontact probe has been calibrated against a contact probe in a tissue-like phantom solution and human muscle tissues; flow changes concurrently measured by the two probes are highly correlated in both phantom ($R^2 = 0.89$, $p < 10^{-5}$) and real-tissue ($R^2 = 0.77$, $p < 10^{-5}$, $n = 9$) tests. The noncontact DCS holds promise for measuring blood flow in vulnerable (e.g., pressure ulcer) and soft (e.g., breast) tissues without distorting tissue hemodynamic properties. © *2012 Society of Photo-Optical Instrumentation Engineers (SPIE).* [DOI: 10.1117/1.JBO.17.1.010502]

Keywords: noncontact; diffuse; correlation; spectroscopy; deep tissue; blood flow.

Paper 11603L received Oct. 14, 2011; revised manuscript received Dec. 1, 2011; accepted for publication Dec. 1, 2011; published online Feb. 3, 2012.

Blood flow is a crucial factor affecting the delivery of oxygen to tissues. Many diseases such as stroke, pressure ulcer, and cancer are associated with abnormal blood flow. Near-infrared (NIR) diffuse correlation spectroscopy (DCS) is an innovative method which can noninvasively probe deep tissue blood flow.[1–7] DCS offers several attractive new features such as noninvasiveness, portability, high temporal resolution, and relatively large penetration depth up to centimeters. DCS measurements of relative blood flow (rBF) changes have been validated against many other standards.[2–4]

Most previous studies with DCS have measured rBF using fiber-optic probes placed on tissue surfaces.[1,3,4,6,7] Significant problems with contact measurements include the risk for infection of vulnerable tissues (e.g., pressure ulcer) and the deformation of soft tissues (e.g., breast) distorting tissue blood flow. Only a few studies have used noncontact DCS probes to monitor rBF in murine tumors[2] or rat brains.[5] In these studies, a probe head bundled with source and detector fibers was mounted at the imaging plane of a conventional camera which was fixed at a distance of ~150 mm from the tissue surface.[2,5] The source and detector fibers were then projected on the tissue surface by the camera lenses aligned in a single optical path for both light delivery and detection. The shared optical path, however, may result in the source light being reflected (by the camera lenses and lens mount) directly into the detector, thus affecting DCS measurement. Although crossed polarizers can be used to reduce the light reflection,[2,5] they substantially attenuate the light intensity, thus reducing signal-to-noise ratio (SNR). Furthermore, the maximum source-detector (S-D) separation was limited by the apertures of camera lenses and the numerical apertures (NA) of optical fibers, and generally less than 10 mm.[2,5] Based on diffusion theory, light penetration depth in tissue is equal to no more than ~1/2 of the S-D separation.[1–6] Therefore, the maximum probing depth of previous noncontact DCS measurements was less than 5 mm.[2,5] For human studies,[3,4,6,7] however, larger S-D separations (e.g., centimeters) are needed to probe deeper tissues (e.g., breast and skeletal muscle). In the present study, we designed a noncontact DCS probe with two separated/isolated optical paths for source and detector respectively. This unique design enabled us to set large S-D separations as needed (e.g., ≥25 mm). The noncontact probe was then calibrated in a liquid phantom solution and in human muscle tissues, against a contact probe validated previously.[3,4]

Figure 1 shows a schematic (a) and a photo (b) of the designed noncontact probe with two optical paths. The source path consisted of a 50 mm focal-length (FL) lens for collimating the source fiber tip and a 250 mm FL lens for focusing the light on the tissue surface. The image spot diameter of the projected source fiber (diameter = 200 μm) through this source path was ~1.3 mm, which efficiently lowered down the illumination density to ensure skin safety. The detector path used a 0.16 NA collimator (780 nm aligned, Edmund Optics, NJ) for collimating the detector fiber tip and a 200 mm FL lens for focusing. A long-pass optical filter (>750 nm, Thorlabs, NJ) and an aperture were installed in the detector path to attenuate the ambient light and stray photons. The lenses used were achromatic doublet lenses (diameter = 25.4 mm) with antireflection coated at the range of 650 to 1050 nm (Thorlabs, NJ). All optical components were mounted on mechanical cages (Thorlabs, NJ). Two optical paths were covered and isolated with crepe black weave (Altas International, CA) to avoid the interference between the source and detector and to prevent ambient light. By using separated optical paths the source and detector could be easily adjusted and modified individually, e.g., adding the optical filter and aperture in the detector path without attenuating light in the source path. This dual-path design also avoided using expensive components required for the single-path design with large S-D separations such as polarizers, optical fibers with low NA, and lenses with large aperture and high quality antireflection coating.

The working distance between the noncontact probe and target surface was ~195 mm. The S-D separation was initially set at 26 mm, which can then be easily varied by adjusting the off-axis distance of the source fiber tip. In addition, multiple S-D separation measurements can be achieved by replacing the single source fiber with multiple source fibers placed at different off-axis locations. The S-D fibers [Fig. 1(a)] were connected to a portable DCS device that has been described in detail elsewhere.[2,5,7] Briefly, long-coherence (>5 m) NIR light (785 nm) emitted from a laser diode (100 mw, Crystalaser, CA) enters the tissue via a multimode source fiber

Address all correspondence to: Guoqiang Yu, Center for Biomedical Engineering, University of Kentucky, Lexington, Kentucky, 40506. Tel: 8593237330; Fax: 859257185689; E-mail: guoqiang.yu@uky.edu

0091-3286/2012/$25.00 © 2012 SPIE

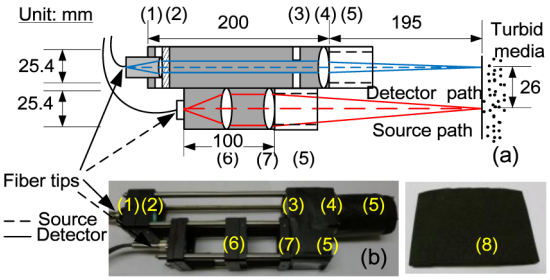

Fig. 1 Schematic (a) and photograph (b) of the noncontact probe including (1) collimator, (2) longpass optical filter, (3) aperture, (4) 200 mm FL lens, (5) protection tube, (6) 50 mm FL lens, (7) 250 mm FL lens and (8) crepe black weave.

(WF200/220/245, Ceramoptec, MA). The scattered light through the tissue is collected by a single-mode detector fiber (SM800-5.6-125, Fibercore, CA) connected to an avalanche photodiode (APD, PerkinElmer, CA). The light intensity fluctuations within a single speckle area of tissue detected by the APD are sensitive to the motion of moving red blood cells in tissue microvasculature. An autocorrelator (Correlator.com, NJ) reads the APD output and computes the temporal light intensity autocorrelation function. Flow index is extracted by fitting the autocorrelation curve, whose decay rate depends on a parameter α (proportional to the tissue blood volume fraction) as well as the motion of the red blood cells.[1–7]

To calibrate the noncontact probe, we conducted concurrent measurements using both contact and noncontact probes (with identical S-D separation of 26 mm) in a tissue-like liquid phantom [Fig. 2(a)] and human muscles [Fig. 2(b)], respectively. The liquid phantom provides a homogeneous tissue model for probe calibration while the use of human muscles allows probe evaluation in real tissues. The liquid phantom is comprised of distilled water, India ink, and Intralipid (30%, Fresenius Kabi, Sweden), which has been commonly used for the calibration of DCS techniques.[1,5,7] India ink is used to manipulate the absorption coefficient μ_a while Intralipid provides particle Brownian motion (flow) and control of the reduced scattering coefficient μ_s'. In this study we set $\mu_a = 0.04$ cm^{-1} and $\mu_s' = 11$ cm^{-1} at 785 nm to mimic the property of real tissue. When using liquid phantom with Intralipid particles to provide Brownian motion, the flow index measured by DCS is expected to be equivalent to the conventional Brownian diffusion coefficient predicted by Einstein.[7] Based on the Einstein—Stocks

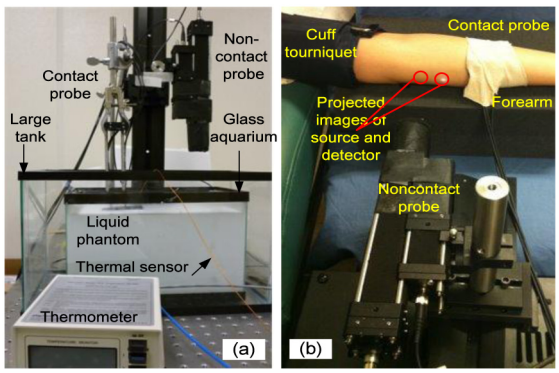

Fig. 2 Experimental setup for concurrent flow measurements using contact and noncontact probes in a liquid phantom solution (a) and a forearm muscle (b).

equation,[8] the Brownian motion of particles inside liquid phantom is positively proportional to phantom temperature. Therefore, we created flow index variations by changing the phantom temperature for the calibration of noncontact DCS flow measurements.

Setup for the liquid phantom experiment is shown in Fig. 2(a). A contact probe was placed on the surface of liquid phantom solution contained inside a glass aquarium to simulate a semi-infinite geometry. A noncontact probe was held by a custom-made holder above and perpendicular to the phantom surface. The two probes were connected respectively to two DCS devices that acquired flow data alternatively. A thermometer sensor (Physitemp, NJ) was placed between the two probes at a distance of ~15 mm beneath the phantom surface for temperature measurement. Phantom temperature was changed by filling hot water twice into a large tank that contained the glass aquarium with phantom solution [Fig. 2(a)]. Room light was turned off during measurements although it did not show significant influences on the coherence factor, SNR, and flow index. Figure 3(a) shows the relative flow changes during temperature variations. DCS flow data were normalized to their baseline value (assigned 100%) at the beginning of the experiment. As expected, the flow changes followed the temperature variations in a linear pattern [Fig. 3(b)]. The percentage flow changes measured by the two probes are highly correlated ($R^2 = 0.89$, $p < 10^{-5}$) and demonstrate an excellent linear relationship (regression slope = 1.00, interception = 1.29).

Validation measurements in human muscles were approved by the University of Kentucky Institutional Review Board. Nine healthy volunteers participated in this study. Each subject was asked to lay supine and extend his/her forearm. The forearm was gently fixed on the bed using elastic belts, and kept relatively static. The contact/noncontact probe was taped/projected on an adjacent area of the left forearm flexor muscle whose surface was relatively flat [Fig. 2(b)]. An arterial cuff-occlusion paradigm was applied on the upper arm to induce blood flow changes in forearm muscles. The experimental protocol included 5 min baseline, 5 min cuff inflation (230 mm Hg), and 5 min recovery following the deflation. Room light was turned off during measurements to minimize the influence. Similarly, rBF was calculated by normalizing flow indices to their baseline value (assigned 100%) before occlusion. Figure 4 shows rBF responses during occlusion in one typical subject (a) and over nine volunteers (b). As expected, significant correlations between the contact and noncontact measurements were observed in the single subject [$R^2 = 0.94$, $p < 10^{-5}$, see Fig. 4(c)] and over the nine volunteers [$R^2 = 0.77$, $p < 10^{-5}$,

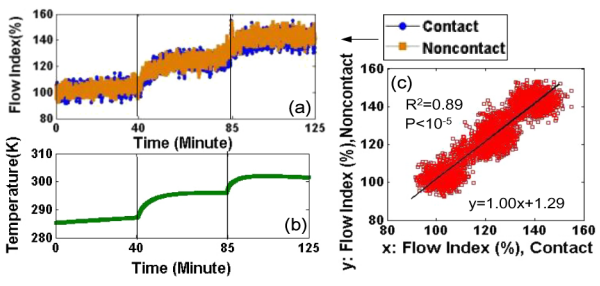

Fig. 3 Relative flow changes (a) measured by the contact and noncontact probes during temperature variations (b) are highly correlated (c). The vertical lines in (a) and (b) represent the time points to fill hot water (twice) into the large tank [see Fig. 2(a)].

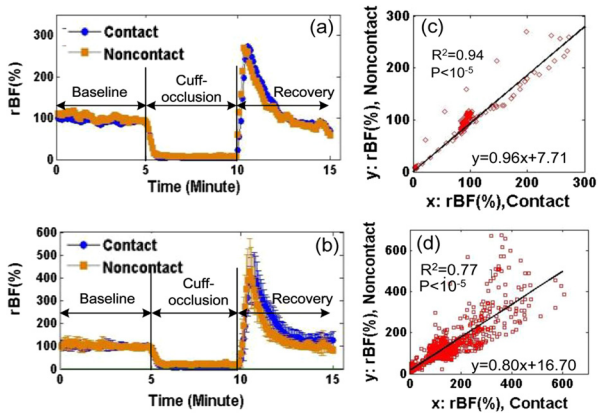

Fig. 4 Forearm muscle rBF responses during 5-minute arterial occlusion in one typical subject (a) and over 9 volunteers (b). The average rBF over 9 subjects (b) are illustrated as mean ± standard deviation (error bar). Significant correlations between the contact and noncontact flow measurements are observed in the single subject (c) and over the 9 volunteers (d).

see Fig. 4(d)]. We notice that the regression slope (0.80) and interception (16.70) over subjects [Fig. 4(d)] are slightly different from the expected values (1 and 0 respectively). The discrepancies between the two measurements (especially during the recovery phase) may result from tissue heterogeneous responses as well as differences in measurement technique. For example, the noncontact measurement may be influenced by stray light as well as the light reflected directly from forearm skin surface (without going through the deep tissue) while the contact measurement may be influenced by the imperfect probe-tissue coupling and the contact pressure distorting tissue blood flow.[4] Further comparisons with other flow measurement standards are needed to identify these influence factors.

To conclude, we have produced a novel design of a noncontact DCS probe for deep tissue blood flow measurement. Two separated optical paths are used for source and detector respectively, which avoids the interference between the source and detector, and enables the setting of large S-D separations for deep tissue flow detection. The noncontact probe has been calibrated against a validated contact probe in a liquid phantom solution and human tissues, and good agreements in flow measurements are found. The noncontact design makes it possible to use this technology for detecting blood flow in vulnerable (e.g., pressure ulcer) and soft (e.g., breast) tissues without distorting tissue hemodynamics.

Acknowledgments

The authors thank funding support from the National Institutes of Health (NIH) R01 CA149274 and NIH National Center for Research Resources (NCRR) UL1RR033173.

References

1. D. A. Boas, L. E. Campbell, and A. G. Yodh, "Scattering and imaging with diffusing temporal field correlations," *Phys. Rev. Lett.* **75**(9), 1855–1858 (1995).
2. G. Yu et al., "Noninvasive monitoring of murine tumor blood flow during and after photodynamic therapy provides early assessment of therapeutic efficacy," *Clin. Cancer Res.* **11**(9), 3543–3552 (2005).
3. M. N. Kim et al., "Noninvasive measurement of cerebral blood flow and blood oxygenation using near-infrared and diffuse correlation spectroscopies in critically brain-injured adults," *Neurocrit. Care* **12**(2), 173–180 (2010).
4. G. Yu et al., "Validation of diffuse correlation spectroscopy for muscle blood flow with concurrent arterial spin labeled perfusion MRI," *Opt. Exp.* **15**(3), 1064–1075 (2007).
5. C. Cheung et al., "In vivo cerebrovascular measurement combining diffuse near-infrared absorption and correlation spectroscopies," *Phys. Med. Biol.* **46**(8), 2053–2065 (2001).
6. Y. Shang et al., "Portable optical tissue flow oximeter based on diffuse correlation spectroscopy," *Opt. Lett.* **34**(22), 3556–3558 (2009).
7. D. Irwin et al., "Influences of tissue absorption and scattering on diffuse correlation spectroscopy blood flow measurements," *Biomed. Opt. Exp.* **2**(7), 1969–1985 (2011).
8. G. Peskir, "On the diffusion coefficient: the Einstein relation and beyond," *Stoch. Models* **19**(3), 383–405 (2003).